Am J Cancer Res 2023;13(5):1845-1862
www.ajcr.us /ISSN:2156-6976/ajcr0148975

Original Article

ANO10 is a potential prognostic biomarker and correlates with immune infiltration in breast cancer

Ran Ning[1], Shuaikang Pan[2,3], Dashu Xiao[1], Yan Zheng[1], Jinguo Zhang[2]

[1]Department of Pathology, The Affiliated Chaohu Hospital of Anhui Medical University, Chaohu 238000, Anhui, China; [2]Department of Medical Oncology, The First Affiliated Hospital of USTC, Division of Life Science and Medicine, University of Science and Technology of China, Hefei 230000, Anhui, China; [3]School of Medical Oncology, Wan Nan Medical College, Wuhu 241000, Anhui, China

Received January 5, 2023; Accepted April 13, 2023; Epub May 15, 2023; Published May 30, 2023

Abstract: Several diseases have been linked to the dysfunction of anoctamins. Anoctamins play a wide range of physiological roles, including cell proliferation, migration, epithelial secretion, and calcium-activated chloride channel activity. However, the function of anoctamin 10 (ANO10) in breast cancer is still unclear. ANO10 was highly expressed in bone marrow, blood, skin, adipose tissue, thyroid gland and salivary gland, while ANO10 was expressed at low levels in liver and skeletal muscle. Compared to benign breast lesions, the protein level of ANO10 was lower in malignant breast tumors. However, breast cancer patients with low ANO10 expression have favorable survival outcomes. ANO10 was negatively correlated with the infiltration of memory CD4 T cells, naïve B cells, CD8 T cells, chemokines and chemokine receptors. Furthermore, the ANO10 low expression group was more sensitive to certain chemotherapy drugs, including bleomycin, doxorubicin, gemcitabine, mitomycin and etoposide. Altogether, ANO10 is a potential biomarker that can effectively predict the prognosis of breast cancer. Our findings highlight the promising prognostic value and therapeutic target of ANO10 in breast cancer.

Keywords: Anoctamin 10, breast cancer, prognostic biomarker, immune infiltration, immune microenvironment

Introduction

Globally, breast cancer (BC) is the most common malignant cancer among women and poses a major burden on the health of the world's population [1]. Despite substantial improvements in diagnosis and treatment, the currently existing therapies remain unsatisfactory for improving the therapeutic efficacy of BC, especially triple-negative breast cancer (TNBC) [2, 3]. Previous genomic discoveries have led to the identification of four molecular intrinsic subtypes of BC (Luminal A, Luminal B, HER2-enriched and Basal-like), which are associated with different clinical outcomes and treatment selection [4, 5]. Beyond that, although most BCs are curable with current treatment options if detected early enough, approximately 20% of patients will have early relapses within 10 years [6]. In general, biomarkers are objective measures of a biological system's current condition, assisting in identifying the progression and therapy responses of BC [7, 8]. Prognostic biomarkers can be used to identify which patients will benefit from specific therapies [9]. Additionally, an increasing number of BC patients are seeking personalized or unique treatments, which facilitate the development of novel biomarkers for early diagnosis, treatment and prognostic assessment of BC [10, 11]. In recent years, significant progress has been made in the field of biomarkers in BC. Several multigene indicators, such as MammaPrint and Oncotype DX, have been used to predict prognosis and benefit from chemotherapy in BC patients [12, 13].

In recent years, cancer immunotherapies have achieved remarkable success and have become the fourth bell mode following surgery, chemotherapy and radiotherapy [14, 15]. In the past, BC was considered a low immunogenic cancer due to a low tumor mutational burden and a limited ability to form tumor neoantigens

and, therefore, was not appropriate for immunotherapies [16]. However, increasing evidence suggests a strong connection between BC and the immune system [17]. According to large clinical studies, immune checkpoint inhibitors (ICIs), such as pembrolizumab and atezolizumab, are efficacious for early-stage or metastatic TNBC [18, 19]. However, individual responses to ICIs vary greatly in terms of both efficacy and toxicity for BC patients. Moreover, several anti-tumor immune therapies for BC are still in their early clinical phases of development. Therefore, identifying, validating, and utilizing reliable biomarkers of response to immunotherapies are warranted.

The anoctamin family (also known as TMEM16) includes 10 transmembrane proteins (ANO1-10), which have been linked to various diseases and cancer [20]. Human anoctamin proteins were reported to have multiple functions, including calcium-activated chloride channel activity and phospholipid scrambling activity [21, 22]. It has been shown that anoctamins play a significant role in a variety of physiological processes including ciliogenesis [23], cell cycle progression [24], inflammatory response [25], esophageal epithelial proliferation [26] and osteoclast differentiation [27]. However, the function of ANO8 and ANO10 remains not to be fully elucidated. Researchers have found that ANO10 exhibits both calcium-dependent chloride channel activity and phospholipid scrambling activities [28, 29]. ANO10 scrambling activity has been linked to lipid metabolism in the endoplasmic reticulum membrane [30]. ANO10 mutation leads to neurological defects and abrogated ion transport [31, 32]. However, to date, the role of ANO10 in BC and antitumor immunity remains obscure.

In this study, we systematically investigated the multiple roles of ANO10 in BC. To this end, the expression of ANO10 was analyzed in The Cancer Genome Atlas (TCGA) database and paraffin tissue sections from BC patients. The prognostic value of ANO10 in predicting BC patient was also determined. Furthermore, we then assessed the prognostic value of ANO10 in BC. Our analyses revealed a potential relationship between ANO10 and immune cell infiltration in BC. The ANO10 genomic alterations in BC and the effect of ANO10 on drug sensitivity were further determined. Overall, our study provides crucial insight into the roles of ANO10 and highlights the multifaceted function of ANO10 in BC.

Materials and methods

Data collection and preprocessing

Expression data from the GTEx database (https://www.gtexportal.org/home) were used to analyze the expression of ANO10 in normal human tissues. The expression of ANO10 in 31 human normal tissues was extracted via a Perl script. The RNA-seq data of TCGA pan-cancer were accessed using the UCSC Xena browser (https://xena.ucsc.edu/). Statistical comparisons of ANO10 in pan-cancer were performed by the Mann Whitney U test. TCGA breast cancer (BRCA) expression data and clinical data were obtained from the TCGA data portal (https://www.cancer.gov/tcga). TCGA BRCA patients were divided into high expression and low expression groups based on the median expression of ANO10. The UALCAN tool (http://ualcan.path.uab.edu) was applied to investigate the expression of ANO10 in different BC subtypes [33].

Survival analysis of ANO10 in BC

An evaluation of the prognostic value of ANO-10 on survival in BC patients was conducted using the Kaplan-Meier Plotter database (www.kmplot.com) [34]. We investigated the association of ANO10 expression with overall survival (OS) in different BC subtypes. The optimized cut-off values were determined by auto-select best cut-off value. In addition, survival analysis of ANO10 in Gene Expression Omnibus (GEO) datasets was also evaluated via the PrognoScan tool (http://dna00.bio.kyutech.ac.jp/PrognoScan/) [35].

Genomic alterations of ANO10 in BC

We analyzed the genomic profiles of ANO10 in BC using the cBioPortal database (http://www.cbioportal.org/) [36]. The dataset of breast invasive carcinoma (TCGA, Firehose Legacy) was included for our analysis. ANO10 genetic alterations in the TCGA-BRCA dataset were summarized in the “OncoPrint” module. The co-occurrence analysis of ANO10 mutations was performed with the “Comparison/Suvival” module.

Analysis of differentially expressed genes (DEGs)

The expression data of TCGA-BRCA were used to identify DEGs between the high-ANO10 expression subgroup and the low-ANO10 expression subgroup with "limma" R package [37]. The DEGs were defined as those with |log2 (FC)| > 1 and an adjusted *P*-value < 0.05.

Enrichment analysis

Gene Ontology (GO) and Kyoto Encyclopedia of Genes and Genomes (KEGG) pathway analyses were conducted on DEGs. We used the R software package "ClusterProfilter" for enrichment analysis [38]. In multiple GSEA plot analysis, MSigDB category (h.all.v7.5.1.symbols.gmt and c2.cp.kegg.v7.4.symbols.gmt) was set as the reference gene set, which was achieved with the R packages "enrichplot" and "clusterProfiler". Only the top 8 terms are presented here. Statistical significance was determined by a *P*-value < 0.05 and a q-value < 0.25.

Immune infiltration analysis and TISIDB database

In this study, we investigated the association of the expression level of ANO10 with the infiltration levels of immune cells with the CIBERSORT and ESTIMATE algorithms [39, 40]. Spearman's correlation test was used to determine the correlation between ANO10 expression and immune checkpoint genes in BC. The correlations between ANO10 expression and different BC subtypes, chemokine receptors and chemokines were analyzed using TISIDB (http://cis.hku.bhk/TISIDB/) [41].

Drug sensitivity analysis

We used the R package "pRRophetic" to predict chemotherapy sensitivity in BC based on the largest pharmacogenomics database Genomics of Drug Sensitivity in Cancer (GDSC) [42]. To predict the relationship between ANO10 and sensitivity to drugs, we adopted regression methods to estimate the IC50 for each chemotherapeutic drug.

RT-qPCR

Human mammary epithelial cells MCF-10A were cultured in basal medium supplemented with a mammary epithelial growth kit. HCC1937 or MCF-7 cells were cultured in RPMI-1640 media (GIBCO) supplemented with 10% fetal bovine serum (FBS). SKBR3 cells were grown in DMEM (GIBCO) medium supplemented with 10% FBS. Total RNA was extracted from cells with an RNA-Quick Purification Kit (Yishan Biotechnology Co., Ltd.). Reverse-transcription (RT) was performed using Thermo Scientific RevertAid Reverse Transcriptase (Thermo Fisher Scientific, Waltham, MA, USA). Quantitative RT-PCR was performed using a Roche LightCycler 96 with the Universal SYBR Green Fast qPCR Mix (Abclonal, Woburn, MA, USA). The primers sequences used in this study were as follows: Human ANO10 forward, CGTCTGGCATCGTGATTCAG; Human ANO10 reverse, GCAAACCGAGTGTACCAGGT; Human GAPDH forward, GGAGCGAGATCCCTCCAAAAT; Human GAPDH reverse, GGCTGTTGTCATACTTCTCATGG; GAPDH was used as an internal endogenous control.

Immunohistochemical staining (IHC) and analysis

The study on human subjects was approved by the Ethics Committee of Chaohu Hospital of Anhui Medical University (KYXM-202212-011). The benign breast tissue from 12 patients and 40 patients with malignant breast adenocarcinoma tissue at Chaohu Hospital, Anhui Medical University from January, 2017 to October, 2022 were retrieved for the present study. These patients did not receive radiotherapy or chemotherapy before surgery. The 10% formalin-fixed paraffin-embedded breast tissue specimens were obtained and pathologically diagnosed by a clinical pathologist at Chaohu Hospital. The tissue sections were deparaffinized in xylene, and rehydrated in a descending alcohol series. Hydrogen peroxide (3%) was used to quench endogenous peroxide activity for 15 minutes. The sections were blocked with 10% normal goat serum for 40 min at room temperature, and then incubated overnight at 4°C with an anti-ANO10 antibody (1:400 dilution, Proteintech). The following day the tissue sections were incubated with biotinylated anti-rabbit secondary antibody at room temperature for 1 h. Detection of the signal was performed using a DAB kit after washing. The scoring of ANO10 immunoreactive staining was used as described previously [43]. In this

study, we defined cases with IHC scores less than or equal to 5 as low ANO10 staining, IHC scores equal to 6 as moderate ANO10 staining and those with score equal to 7 as strong ANO10 staining. Cases with strong ANO10 staining were classified as the high ANO10 expression group, while others were classified as the low ANO10 expression group.

Statistical analysis

Bioinformatics analysis and plots were generated using software R (version 4.1.2, Vienna, Austria). Student's t-tests were used to compare two groups. For multiple comparisons, one-way ANOVA followed by Tukey test was adopted. The relative mRNA level of ANO10 was calculated using the ($2^{-\Delta\Delta Ct}$) method. Other statistical methods are described above.

Results

Expression levels of ANO10 in normal tissues and cancer

We first investigated the global expression of ANO10 in human normal tissues using the GTEX dataset. As shown in **Figure 1A**, ANO10 was highly expressed in the bone marrow, blood, skin, adipose tissue, thyroid gland and salivary gland, while ANO10 was expressed at low levels in liver and skeletal muscle. In addition, ANO10 expression was higher in adipose tissue, blood vessel and brain in females than in males. However, a higher level of ANO10 in thyroid gland was observed in males than in females (**Figure 1B**). We then explored the mRNA level of ANO10 in pan-cancer using the TCGA database. We found that ANO10 mRNA was differentially expressed in 15 cancer types. As demonstrated in **Figure 1C**, ANO10 expression was significantly higher in cholangiocarcinoma (CHOL), kidney chromophobe (KICH), liver hepatocellular carcinoma (LIHC) and pheochromocytoma and paraganglioma (PCPG). In contrast, ANO10 mRNA was significantly downregulated in breast invasive carcinoma (BRCA), cervical squamous cell carcinoma and endocervical adenocarcinoma (CESC), colon adenocarcinoma (COAD), head and neck squamous cell carcinoma (HNSC), kidney renal clear cell carcinoma (KIRC), kidney renal papillary cell carcinoma (KIRP), lung adenocarcinoma (LUAD), lung squamous cell carcinoma (LUSC), prostate adenocarcinoma (PRAD), rectum adenocarcinoma (READ) and thyroid carcinoma (THCA).

Protein level of ANO10 in human breast cancer

By immunohistochemistry staining, low expression of ANO10 was observed in human breast cancer compared with benign breast lesions that showed moderate and strong staining (**Figure 2A**). IHC staining of ANO10 protein expression in BC was scored as strong staining (5/40), moderate staining (20/40) and low staining (15/40). In contrast, IHC staining of ANO10 protein expression in benign breast lesions was scored as strong staining (9/12), moderate staining (3/12) and low staining (0/12) (**Figure 2B** and **2C**). Based on the IHC score as indicated before, we classified ANO10 expression into low expression and high expression groups (**Table 1**). The expression of ANO10 was obviously different between BC and benign breast lesions. The protein level of ANO10 was significantly lower in BC tissues ($P < 0.001$). However, the protein level of ANO10 was not significantly different with regard to age, tumor size, lymph node metastasis, Ki67 expression and clinical stage.

The mRNA expression and genetic alteration of ANO10 in the TCGA-BRCA cohort

We next focused on the role of ANO10 in BC. As demonstrated in **Figure 3A**, compared to normal breast tissues, the expression of ANO10 was lower in BC subtypes, especially in TNBC. The low expression of ANO10 was significantly associated with a high disease stage (**Figure 3B**). At the genome scale, the ANO10 gene was altered in 53 BC patients, which comprised only 5% across 1098 samples. The most frequent alterations of the ANO10 gene in BC were low mRNA, high mRNA and deep deletion (**Figure 3C** and **3D**). Intriguingly, the co-occurrence of TP53 and OBSCN alterations was observed in the ANO10 alteration group (**Figure 3E**). The results of RT-qPCR demonstrated that ANO10 mRNA was lower in BC cells (HCC1937, MCF7 and SKBR3) than in normal MCF-10A mammary epithelial cells (**Figure 3F**).

Survival analysis of ANO10 in breast cancer

To evaluate the prognostic value of ANO10 in BC, we assessed the associations of ANO10 with clinical survival outcomes with the Kaplan-

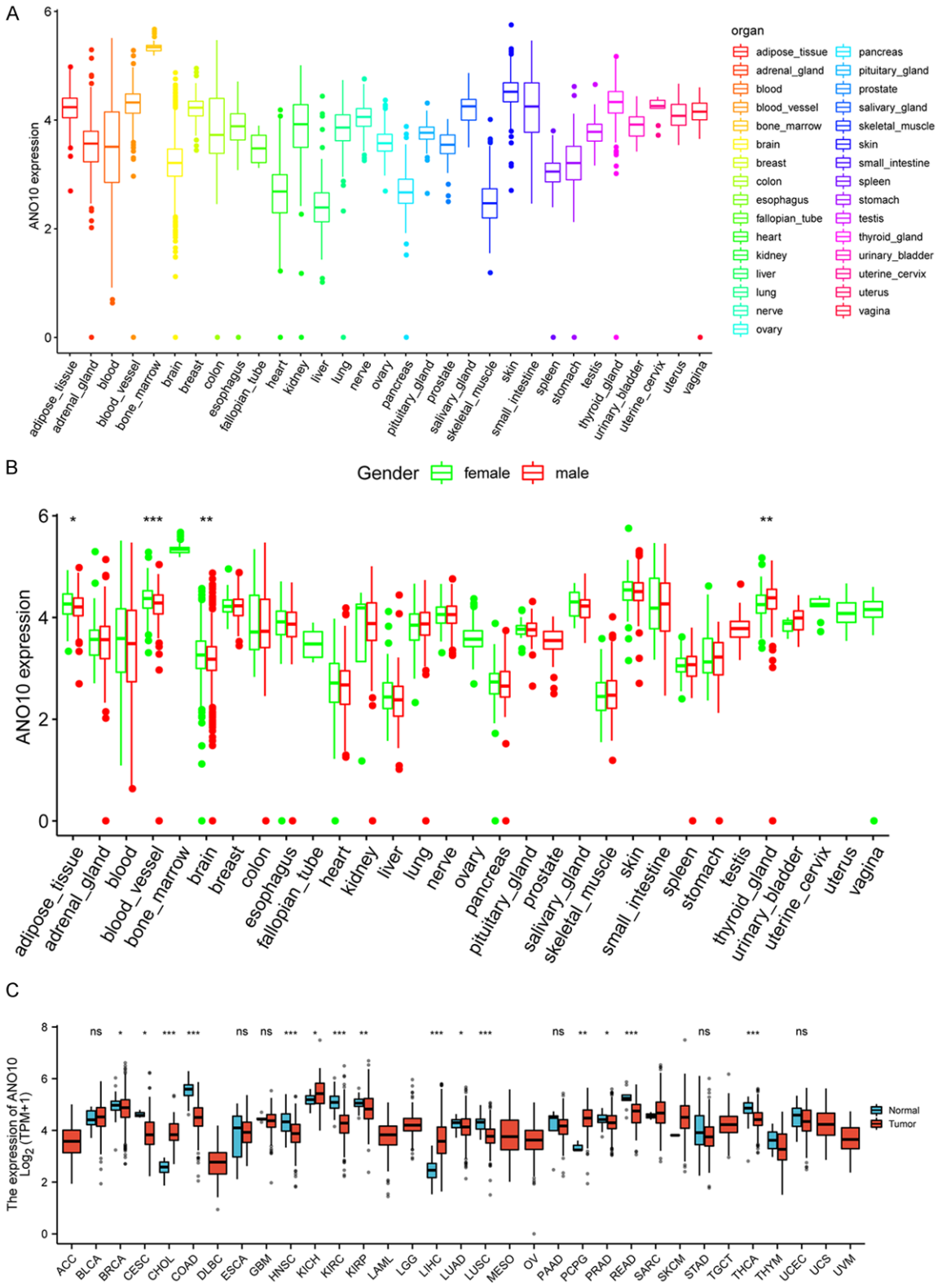

Figure 1. The mRNA level of ANO10 in normal tissues and cancer. A. The mRNA level of ANO10 in normal tissues from Genotype Tissue-Expression (GTEX) data. B. The ANO10 expression abundances of various tissues in males and females. ***, $P < 0.001$. C. Comparison of the mRNA level of ANO10 in 33 TCGA cancers and GTEX normal tissues. The red column represents the cancer samples, and the blue column represents the normal samples. ns, $P \geq 0.05$; *, $P < 0.05$; **, $P < 0.01$; and ***, $P < 0.001$.

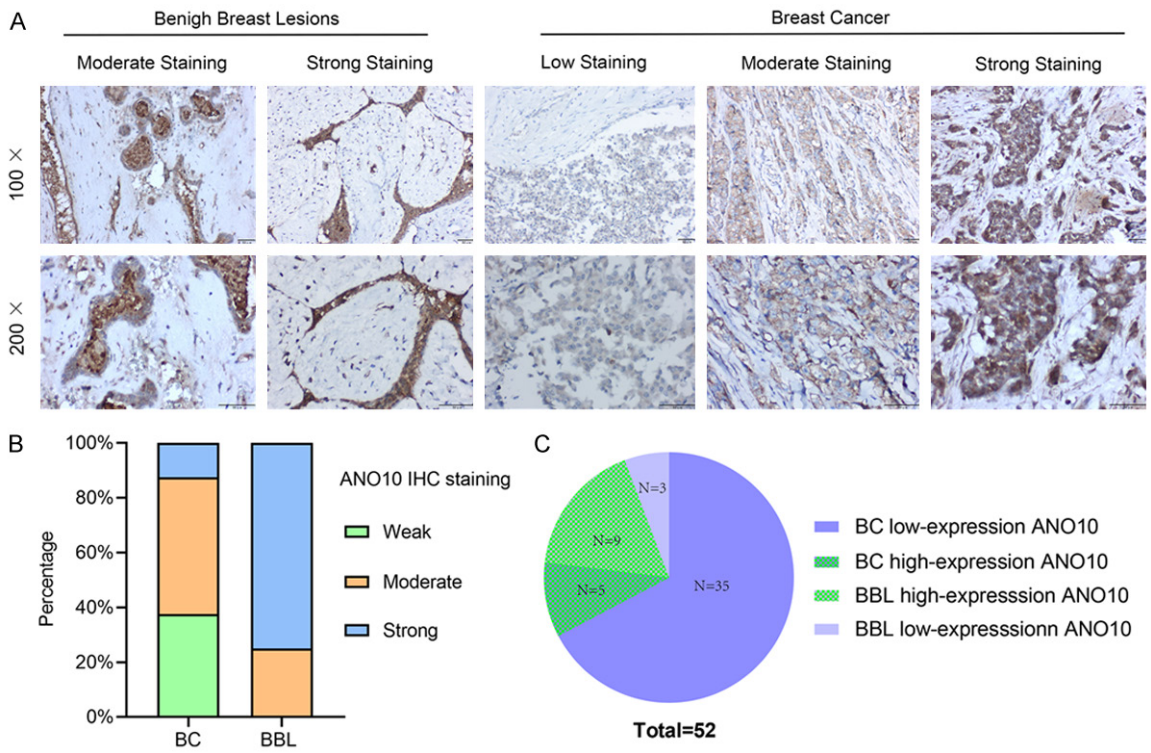

Figure 2. The protein level of ANO10 in human breast cancer detected by IHC. A. Representative pictures of immunohistochemical ANO10 staining patterns in human breast samples (100× magnification and 200× magnification). B. Relative proportion of ANO10 IHC staining in breast cancer and benign breast lesions. C. The pie chart depicts ANO10 to be underexpressed in 87.5% of BC cases compared with 25% with underexpression in benign breast lesions. BC, breast cancer; BBL, benign breast lesions.

Meier plotter online tool. We found that BC patients with low ANO10 expression had a favorable OS (**Figure 4A**). Regarding the prognostic value of ANO10 in different BC subtypes, our results demonstrated that lower expression in Luminal B, HER2-enriched and Basal subtype patients had a better OS compared to those with a higher level of ANO10 (**Figure 4C-E**). A similar result was also observed for distant metastasis-free survival (DMFS) in the basal subtype (**Figure 4F**). However, ANO10 did not show prognostic value for long-term survival in luminal a patients (**Figure 4B**). In addition, the prognostic value of ANO10 in BC was also verified in GEO datasets (GSE4922, GSE1379 and GSE1456, **Figure 4G-I**).

Co-expression and functional enrichment analysis of ANO10

We next screened the genes coexpressed with ANO10. As the circle map shows, ABHD5, APEH, SPCS1, CYB561D2, PSMD6 and ZDHHC3 were positively regulated, while PTBP2, ATXN7L2, ILF3, PRR3 and PRPF38B were negatively regulated (Supplementary Figure 1). We performed differentially expressed gene analysis and found that ACSM1, AKR1D1, TYRP1, etc., were downregulated in the ANO10 low expression group, and APOA2, CKM, COL9A1, etc., were upregulated in the ANO10 low expression group (**Figure 5A** and Supplementary Table 1). We then performed functional enrichment analysis using the differentially expressed ANO10-related genes, including 67 upregulated genes and 623 downregulated genes. The results of GO analysis revealed that DEGs were mainly associated with extracellular structure organization and negative regulation of lipase activity in the BP category, associated with endoplasmic reticulum lumen in the CC category, and related to oxidoreductase activity and DNA-binding transcription activator activity in the MF category (**Figure 5B** and **5C**). The KEGG pathway results showed that the DEGs were involved in neuroactive ligand-receptor

Table 1. Clinicopathological features of patients correlated with ANO10 expression detected by immunohistochemistry

Clinicopathological features	n	ANO10 expression		*P*-value
		Low expression (%)	High expression (%)	
Age at diagnosis				0.308
≤ 50	16	3 (18.8)	13 (18.8)	
> 50	24	22 (91.7)	2 (8.3)	
Histological type				< 0.001[a]
BC	40	35 (87.5)	5 (12.5)	
Benign breast lesions	12	3 (25.0)	9 (75.0)	
Tumor size				0.537[b]
≤ 2 cm	15	12 (80.0)	3 (20.0)	
> 2 cm	25	23 (92.0)	2 (8.0)	
LN metastasis				0.810
YES	22	20 (90.9)	2 (9.1)	
NO	18	15 (83.3)	3 (16.)	
Ki67 expression				0.206
≤ 14%	5	3 (60.0)	2 (40.0)	
> 14%	35	32 (91.4)	3 (8.6)	
Clinical stage				0.258[c]
I+II	31	26 (86.7)	5 (16.1)	
III+IV	9	9 (100.0)	0 (0.0)	

For comparison of ANO10 protein expression associated with age, histological type, tumor size, lymph node metastasis, Ki67 expression, and clinical stage, Fisher's exact test and continuous modified chi-square test were applied. BC, breast cancer; n, number of cases; LN, lymph node. [a]Histological types comparison (BC vs. Benign breast lesions). [b]Tumor size comparison (≤ 2 cm vs. > 2 cm, BC cohort). [c]Clinical stage comparison (I+II vs. III+IV, BC cohort).

interactions, retinol metabolism and cytokine-cytokine receptor interactions (**Figure 5D**). We also conducted single-gene GSEA of ANO10 in BC. As shown in **Figure 5E** and **5F**, ANO10 was mainly enriched in fatty acid metabolism and oxidative phosphorylation in the HALLMARK signature. In addition, ANO10 primarily contributed to lysosomes, metabolism of xenobiotics, and spliceosomes in the KEGG signature. GSEA enrichment analysis of GO terms in ANO10 was shown in Supplementary Table 2.

Correlation between ANO10 and immune cells infiltration

We evaluated the associations of ANO10 immune cell infiltration with the CIBERSORT and ESTIMATE algorithms. We found that the low expression of ANO10 was significantly related to a high Immunescore and ESTIMATE score in BC (**Figure 6A**). The results of CIBERSORT algorithms further demonstrated that the expression of ANO10 was negatively correlated with the infiltration of memory CD4 T cells, naïve B cells and CD8 T cells. A positive relationship was observed between ANO10 expression and M2 macrophages and resting mast cells (**Figure 6B** and **6C**). At the same time, ANO10 expression was negatively correlated with immune checkpoint genes, including PDCD1, TMIGD2, and TNFSF14 (**Figure 6D**). Thorsson et al. developed a pancancer classification that identifies six immune subtypes in TCGA pancancer [44]. Our results indicated that ANO10 expression was lowest in C2 (IFN-γ dominant) and highest in C4 (lymphocyte depleted) immune cell subtypes (Supplementary Figure 2).

Correlation between ANO10 expression and chemokines or chemokine receptors

The inflammatory response is modulated by multiple chemokines, which play an essential role in regulating immune cell infiltration. In this study, we investigated the relationship between ANO10 expression and chemokines using the TISIDB database. Chemokines such as CCL5,

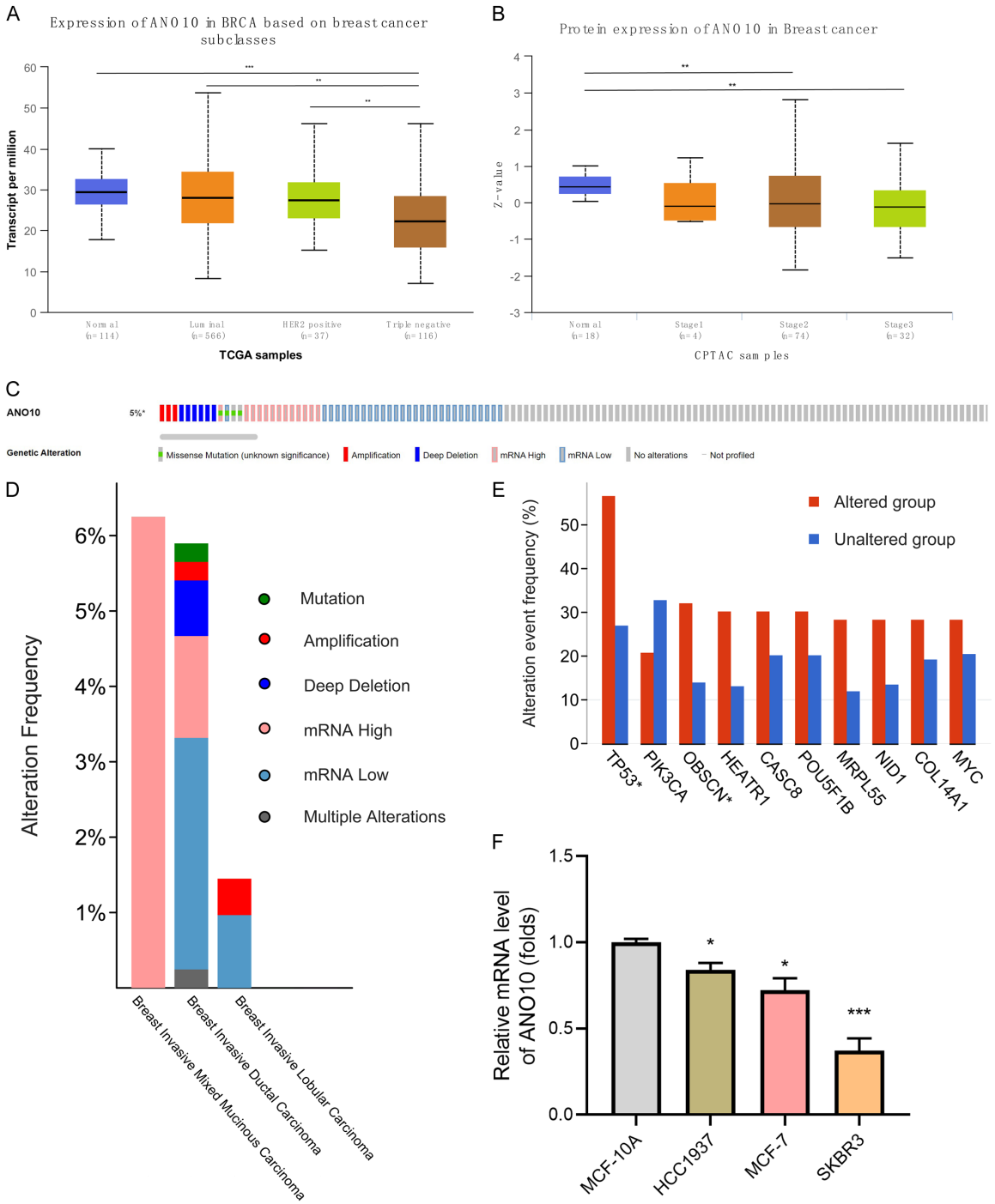

Figure 3. The mRNA expression and genetic alteration of ANO10 in the TCGA-BRCA cohort. A. The transcriptional levels of ANO10 in different BC subtypes. B. The protein level of ANO10 in different stages based on TCGA data. C. OncoPrint visual summary of *ANO10* alterations in the TCGA-BRCA cohort. Five types of genetic alterations were defined: missense mutation (unknown significance), amplification, deep deletion, mRNA high and mRNA low. D. Comprehensive view of the alteration frequency of *ANO10* based on TCGA-BRCA mutation data. E. Analysis of gene mutation cooccurrence comparing the altered group and unaltered group of the *ANO10* gene. F. The mRNA levels of ANO10 in BC cell lines HCC1937, MCF-7 and SKBR3 compared with normal mammary epithelial cells MCF-10A by qRT-PCR. $^{*}P < 0.05$, $^{**}P < 0.01$, $^{***}P < 0.001$.

CCL13, CCL19, CX3CL1, CXCL1, CXCL2, CXCL3 and CXCL5 were negatively correlated with ANO10 expression in BC. In addition, ANO10 was also found to be negatively correlated with

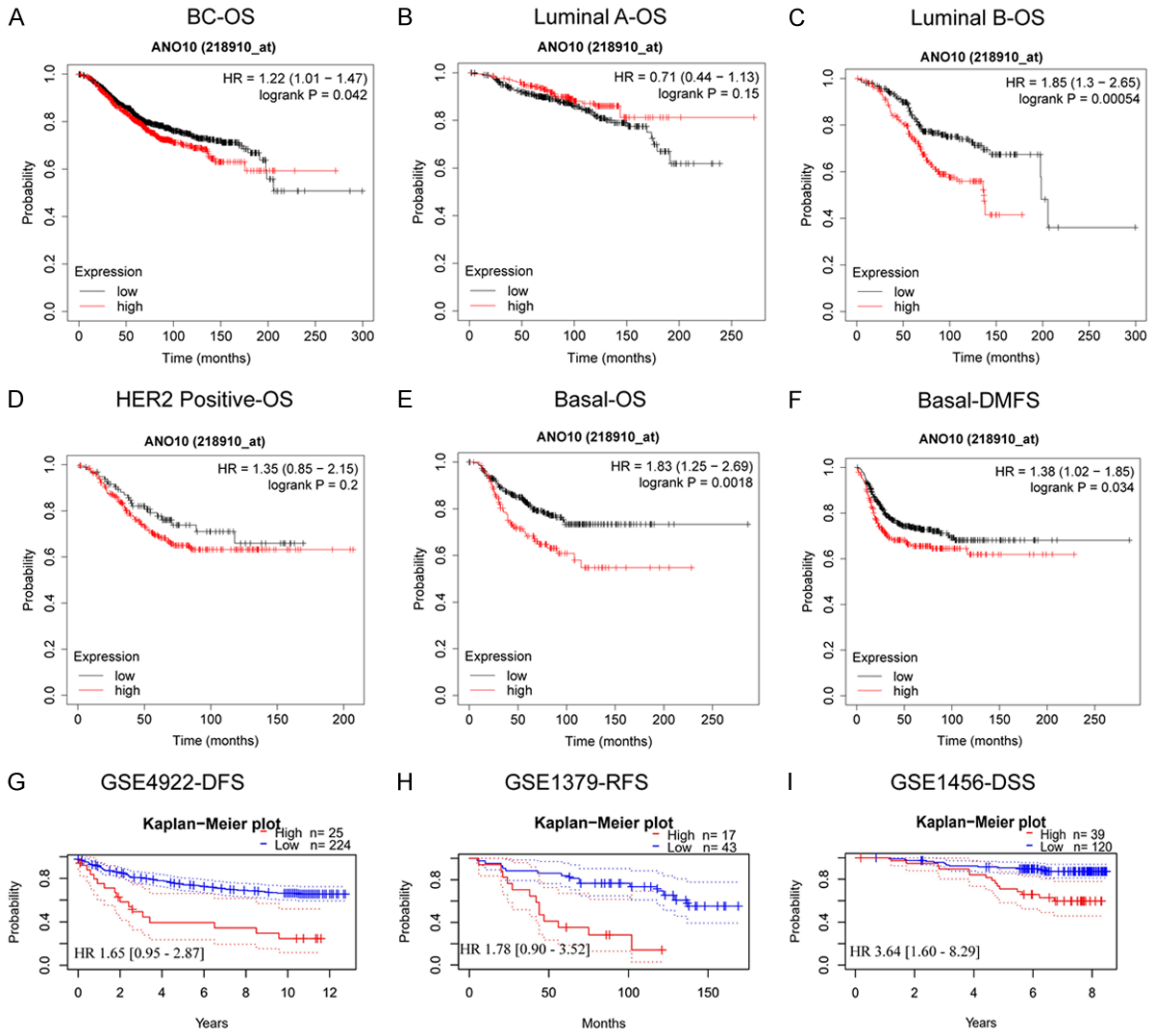

Figure 4. Kaplan-Meier survival curves comparing the high and low expression levels of ANO10. A-E. Kaplan-Meier curves for OS in BC, luminal A subtype of BC, luminal B subtype of BC, HER2 enrichment subtype of BC and basal-like subtype of BC. F. Kaplan-Meier curves for DMFS in the basal-like subtype of BC. G-I. Survival analysis comparing the high to low expression of ANO10 in BC. Data were obtained from the GSE4922, GSE1379 and GSE1456 datasets. DFS, disease-free survival; RFS, recurrence-free survival; DSS, disease-specific survival.

chemokine receptors such as CCR2, CCR4, CCR5, CCR6, CCR7, CXCR3, CXCR5 and CXCR6 (**Figure 7**).

Drug sensitivity analysis of ANO10 in BC

We further explored the underlying chemical compounds sensitive to BC patients with low expression of ANO10 using the GDSC database. The ANO10 low expression group was more sensitive to certain chemotherapy drugs, including bleomycin, doxorubicin, gemcitabine, mitomycin and etoposide (**Figure 8A-E**). Low expression of ANO10 was also more sensitive to certain small molecule inhibitors, such as sunitinib, BMS-754807, Lisitinib and GSK10-70916 (**Figure 8F-I**).

Conclusion

ANO10 is a potential biomarker that can effectively predict the prognosis of BC. ANO10 is expressed at low levels in BC, especially in TNBC. Low expression of ANO10 was associated with a favorable survival outcome of BC. In addition, low expression of ANO10 was negatively correlated with the infiltration of CD8 T cells, chemokines and chemokine receptors. Our findings highlight the promising prognostic value and therapeutic target of ANO10 in BC.

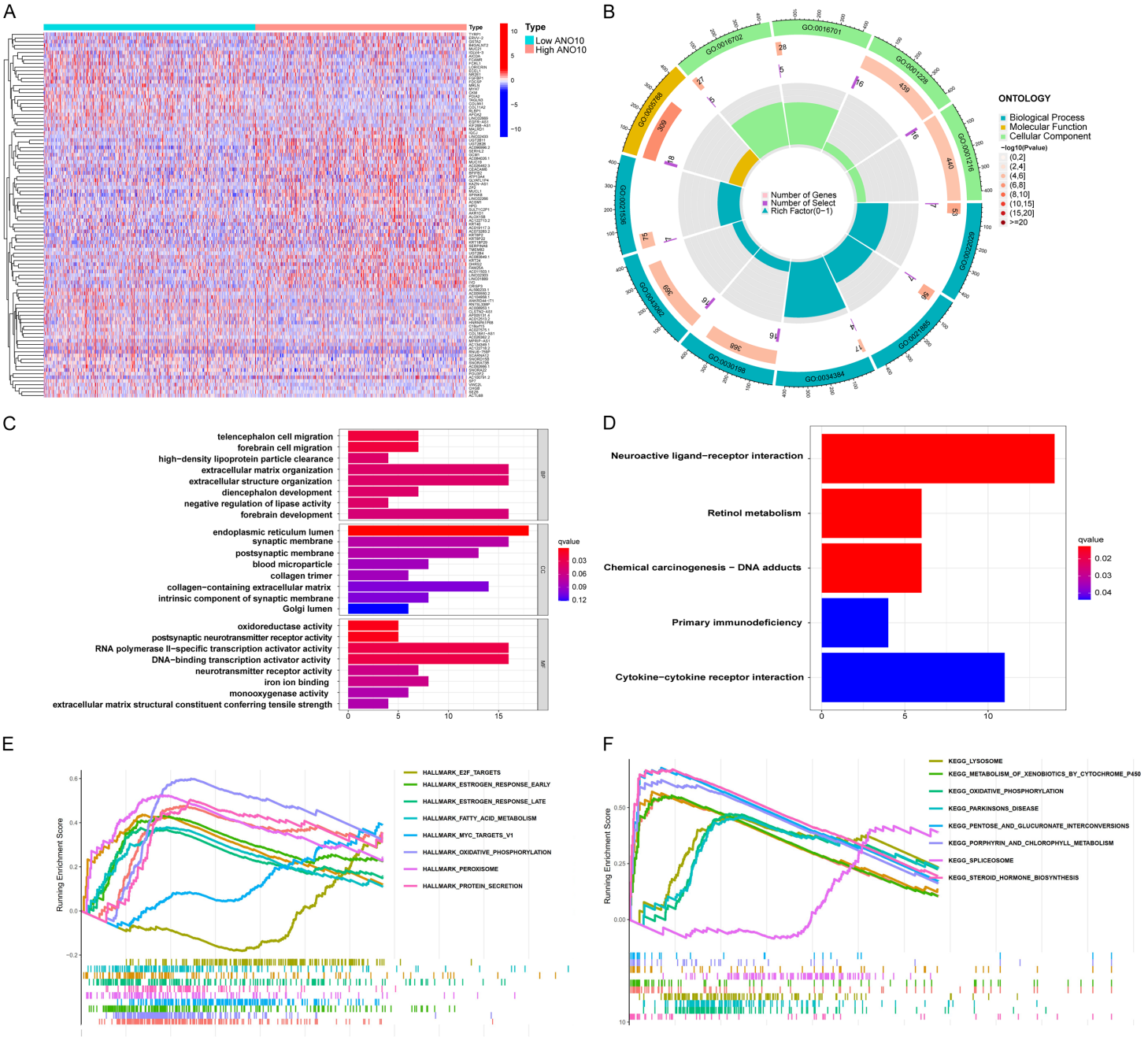
A
Type
Low ANO10
High ANO10
B
ONTOLOGY
Biological Process
Molecular Function
Cellular Component
Number of Genes
Number of Select
Rich Factor(0−1)
C
telencephalon cell migration
forebrain cell migration
high−density lipoprotein particle clearance
extracellular matrix organization
extracellular structure organization
diencephalon development
negative regulation of lipase activity
forebrain development
endoplasmic reticulum lumen
synaptic membrane
postsynaptic membrane
blood microparticle
collagen trimer
collagen−containing extracellular matrix
intrinsic component of synaptic membrane
Golgi lumen
oxidoreductase activity
postsynaptic neurotransmitter receptor activity
RNA polymerase II−specific transcription activator activity
DNA−binding transcription activator activity
neurotransmitter receptor activity
iron ion binding
monooxygenase activity
extracellular matrix structural constituent conferring tensile strength
qvalue
D
Neuroactive ligand−receptor interaction
Retinol metabolism
Chemical carcinogenesis − DNA adducts
Primary immunodeficiency
Cytokine−cytokine receptor interaction
qvalue
E
Running Enrichment Score
HALLMARK_E2F_TARGETS
HALLMARK_ESTROGEN_RESPONSE_EARLY
HALLMARK_ESTROGEN_RESPONSE_LATE
HALLMARK_FATTY_ACID_METABOLISM
HALLMARK_MYC_TARGETS_V1
HALLMARK_OXIDATIVE_PHOSPHORYLATION
HALLMARK_PEROXISOME
HALLMARK_PROTEIN_SECRETION
F
Running Enrichment Score
KEGG_LYSOSOME
KEGG_METABOLISM_OF_XENOBIOTICS_BY_CYTOCHROME_P450
KEGG_OXIDATIVE_PHOSPHORYLATION
KEGG_PARKINSONS_DISEASE
KEGG_PENTOSE_AND_GLUCURONATE_INTERCONVERSIONS
KEGG_PORPHYRIN_AND_CHLOROPHYLL_METABOLISM
KEGG_SPLICEOSOME
KEGG_STEROID_HORMONE_BIOSYNTHESIS

Figure 5. Functional enrichment analysis of ANO10 in BC. A. Heatmap of differentially expressed genes between the low and high ANO10 expression groups. B, C. GO term enrichment analysis of DEG stratification by ANO10 expression. D. KEGG term enrichment analysis of DEG stratification by ANO10 expression. E. GSEA of ANO10-mediated biological processes in the HALLMARK signature. F. GSEA of ANO10-mediated biological processes in the KEGG signature. The curves with different colors indicate the different pathway annotations.

Discussion

In the present study, we aimed to uncover the potential for ANO10 to be utilized as a prognostic biomarker in BC. First, we revealed the expression patterns of ANO10 in human normal tissues and malignant tumors. We found that ANO10 had a high abundance in human bone marrow, thyroid gland and adipose tissue. ANO10 expression sites are closely related to its physiological functions. ANO1 and ANO10 were reported to modulate iodide uptake into thyroid cells via a Na+/I- symporter [45]. Tsuji et al. found that ANO10 rearranges phosphatidylserine in the endoplasmic reticulum membrane and nuclear membrane [30]. Further analysis revealed that ANO10 was abnormally expressed in a variety of human cancers. To date, the anoctamin protein family has rarely been investigated in cancer. The majority of research in the field of the anoctamin protein family in cancer has focused on the ANO1 protein. Functional experiments confirmed that ANO1 served as a tumor oncogene in human gastric cancer and lung cancer [46, 47]. To our knowledge, our study is the first to investigate the role of ANO10 in cancer. Our analysis of the RNA-seq data from TCGA demonstrated that ANO10 mRNA was significantly expressed at low levels in most common cancers, which indicated that ANO10 is a promising biomarker for cancer.

In the present study, we first detected the protein level of ANO10 in BC tissues using IHC staining. Our results demonstrated that lower ANO10 expression was found in BC tissues than in benign breast lesions, indicating that low ANO10 expression may be an important event in BC tumorigenesis. However, ANO10 was not correlated with age, tumor size, lymph node metastasis or stage, which contradicted the TCGA data analysis. The reasons may be due to the small sample size, and larger datasets are needed for future evaluations. We next explored the predictive biomarker role of ANO10 in BC. RT-qPCR experiments demonstrated that ANO10 was downregulated in BC cell lines. From the TCGA data, we found that ANO10 was expressed at low levels in the TNBC subtype and that lower ANO10 levels presented a higher tumor stage, suggesting that reduced ANO10 expression correlated with tumor progression. Regarding the ANO10 genomic alterations in BC, low mRNA and deep deletion were the most common mutation types. A previous study reported that mutations in the ANO10 gene could cause certain diseases or genetic disorders, such as autosomal recessive cerebellar ataxia type 3 [32]. In addition, we found cooccurrence of TP53 alterations with ANO10 alterations. TP53 is the most frequently mutated gene in BC, especially in HER2-positive and TNBC [48]. The above findings indicated that the tumorigenesis of TNBC might be accompanied by mutant ANO10. Our Kaplan-Meier survival analysis revealed that low ANO10 expression could predict a beneficial survival outcome, indicating that ANO10 was a favorable prognostic factor in BC. These results might be interpreted from the point view of immune equilibrium. The low expression of ANO10 may be accompanied by a higher level of immune cell infiltration in the tumor microenvironment. Immune tumor cell infiltration in tumors was correlated with good prognosis for patients [49].

To better elucidate the biological function of ANO10 in BC, we performed GO and KEGG analyses using coexpressed genes of ANO10. The results of the functional analysis of ANO10 revealed that ANO10 was involved in the regulation of lipase activity, extracellular structure organization and membrane-related function. ANO10 was reported to rearrange phosphatidylserine of the endoplasmic reticulum and nuclear membrane in the presence of calcium [30]. ANO10 was also found to correlate with the microtubules of assembling spindles and chromosome segregation [50]. By analyzing KEGG pathways, we found that ANO10 participated in cytokine-cytokine receptor interactions, indicating that ANO10 might be involved in the regulation of the tumor microenvironment. Furthermore, our study demonstrated

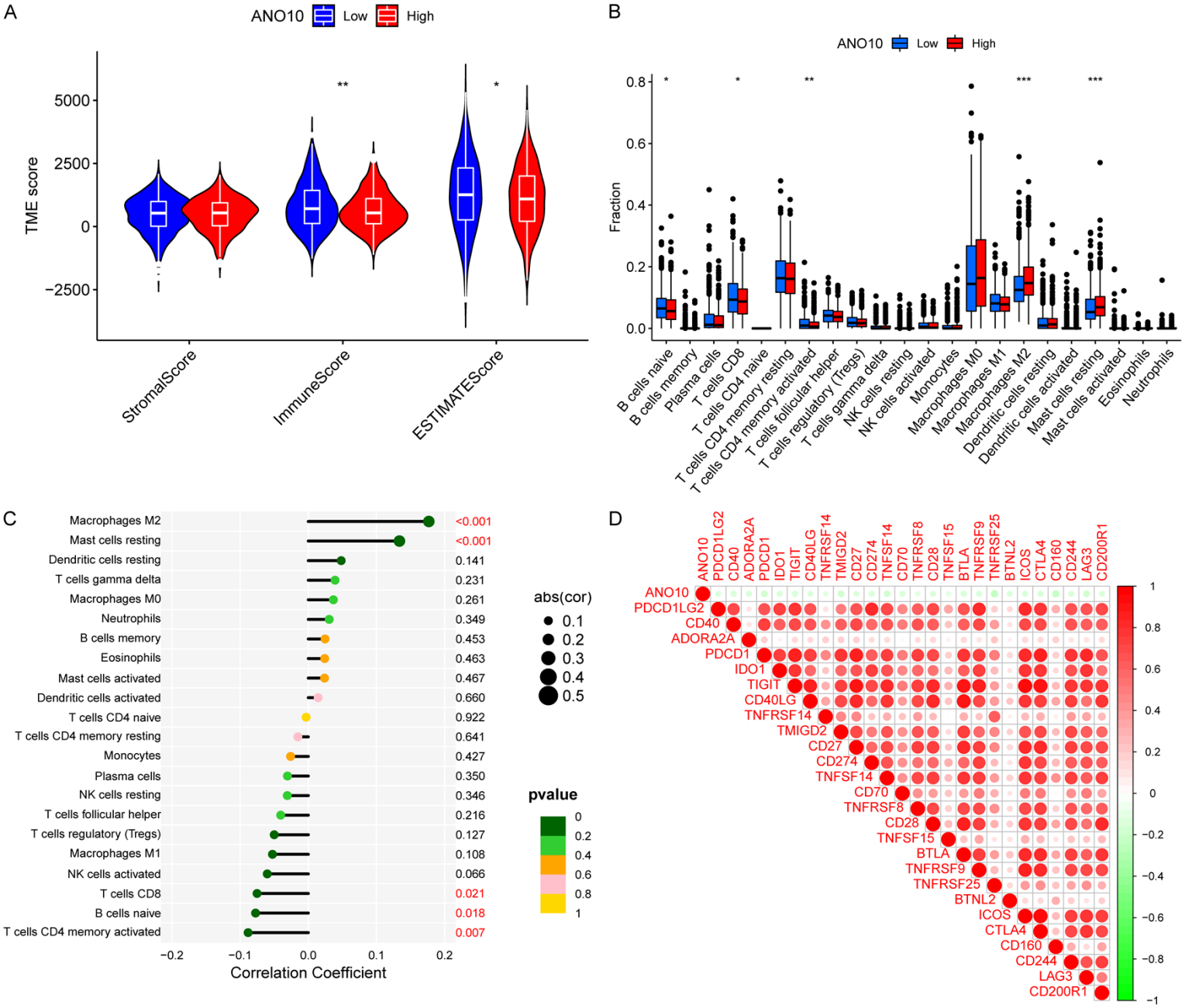
A
ANO10 Low High
TME score
5000
2500
0
−2500
**
*
StromalScore
ImmuneScore
ESTIMATEScore
B
ANO10 Low High
Fraction
0.8
0.6
0.4
0.2
0.0
*
*
**
***
***
B cells naive
B cells memory
Plasma cells
T cells CD8
T cells CD4 naive
T cells CD4 memory resting
T cells CD4 memory activated
T cells follicular helper
T cells regulatory (Tregs)
T cells gamma delta
NK cells resting
NK cells activated
Monocytes
Macrophages M0
Macrophages M1
Macrophages M2
Dendritic cells resting
Dendritic cells activated
Mast cells resting
Mast cells activated
Eosinophils
Neutrophils
C
Macrophages M2 <0.001
Mast cells resting <0.001
Dendritic cells resting 0.141
T cells gamma delta 0.231
Macrophages M0 0.261
Neutrophils 0.349
B cells memory 0.453
Eosinophils 0.463
Mast cells activated 0.467
Dendritic cells activated 0.660
T cells CD4 naive 0.922
T cells CD4 memory resting 0.641
Monocytes 0.427
Plasma cells 0.350
NK cells resting 0.346
T cells follicular helper 0.216
T cells regulatory (Tregs) 0.127
Macrophages M1 0.108
NK cells activated 0.066
T cells CD8 0.021
B cells naive 0.018
T cells CD4 memory activated 0.007
−0.2 −0.1 0.0 0.1 0.2
Correlation Coefficient
abs(cor)
0.1
0.2
0.3
0.4
0.5
pvalue
0
0.2
0.4
0.6
0.8
1
D
ANO10
PDCD1LG2
CD40
ADORA2A
PDCD1
IDO1
TIGIT
CD40LG
TNFRSF14
TMIGD2
CD27
CD274
TNFSF14
CD70
TNFRSF8
CD28
TNFSF15
BTLA
TNFRSF9
TNFRSF25
BTNL2
ICOS
CTLA4
CD160
CD244
LAG3
CD200R1
1
0.8
0.6
0.4
0.2
0
−0.2
−0.4
−0.6
−0.8
−1

Figure 6. Analysis of the associations of ANO10 with immune cell infiltration. A. The distribution of ImmuneScore, StromalScore and ESTIMATEScore in the low and high ANO10 expression subgroups. B. The abundance of each infiltrating immune cell in the low and high ANO10 expression subgroups. The lines in the boxes are the median values. The top and bottom ends of the boxes show the interquartile range of values ($^{*}P < 0.05$; $^{**}P < 0.01$, $^{***}P < 0.001$). C. Lollipop diagrams show the correlation between ANO10 expression and immune cell infiltration. D. Correlations of ANO10 expression and immune checkpoint genes.

that ANO10 was associated with the degree of immune infiltration in BC. To date, the underlying role of anoctamin in the regulation of the immune response remains ill defined. One study reported that high ANO1 was significantly negatively correlated with immune infiltrate in colorectal cancer [51]. A publicly available independent study confirmed that ANO1 is negatively correlated with immune infiltration in gastrointestinal stromal tumors [52]. Jiraporn et al. found that activation of ANO6 was able to affect essential macrophage functions, including migration, phagocytosis of bacteria and bacterial killing [53]. In a previous study, Christian et al. reported that ANO10 promoted the migration of macrophages and phagocytosis of spirochetes, demonstrating that ANO10 plays a central role in innate immune defense against Borrelia infection [54]. In this study, our results indicated that ANO10 was positively correlated with the infiltration of M2 macrophages and resting mast cells. The results were consistent with those previously reported. It has been demonstrated that the chemokine/chemokine receptor system plays a key role in the recruitment of immune cells and inflammation [55]. ANO1-expressing tumor cells promote interleukin 1β secretion to activate NFκB signaling in fibroblasts, stimulate production of the chemokine CCL1 and thus facilitate metastasis of cancer cells [56]. Our findings revealed that ANO10 was negatively correlated with some chemokines/chemokine receptors, suggesting that ANO10 might take part in altering the tumor microenvironment by affecting the secretion of chemokines. It is becoming increasingly evident that immune checkpoint inhibitors (ICIs) are the most effective immunotherapeutic approach for treating cancer [16]. In this study, we also explored the relationship between ANO10 and checkpoint genes. We found that low expression of ANO10 was associated with high expression of checkpoint genes, indicating that low ANO10 expression might be an indicator of immune escape and is suitable for ICI therapy. To further elucidate the immunosuppressive role of low ANO10 expression, we explored the relationship between ANO10 expression and chemokines and chemokine receptors in TNBC. Our results demonstrated that ANO10 was negatively correlated with chemokines and chemokine receptors. To date, the regulation of ANO10 in chemokines has not been reported in the literature. However, knockdown of ANO6 was reported to reduce the chemokine-induced migration of dendritic cells [57]. We then performed drug sensitivity analysis to identify potential target molecular compounds. Our results demonstrated that the IC50 of the ANO10 low expression group was lower than that of the high expression group for some chemotherapy drugs, suggesting that patients with low expression of ANO10 may benefit from chemotherapy. Chemotherapy can stimulate immune responses by increasing the antigenicity of cancer cells or enhancing their adjuvant properties, which has been defined as a potential immunogenic cell death mechanism [58, 59]. Overall, our data revealed that low expression of ANO10 was more suitable for immunotherapy and chemotherapy.

To our knowledge, our study is the first to explore the clinical significance of ANO10 in BC patients. However, this study still has some limitations, and future research needs to address these limitations. The sample size is relatively small, and further studies need to verify our conclusions by expanding the sample size in the future. Regarding the role of ANO10 in immune infiltration, we only performed correlation analyses, and experimental validation of the molecular mechanisms underlying these correlations is still needed.

Acknowledgements

This work was supported by grants from Scientific Research Start-up Funds of The First Affiliated Hospital of USTC (RC2021122) and China Postdoctoral Science Foundation (2022M723048) to JZ.

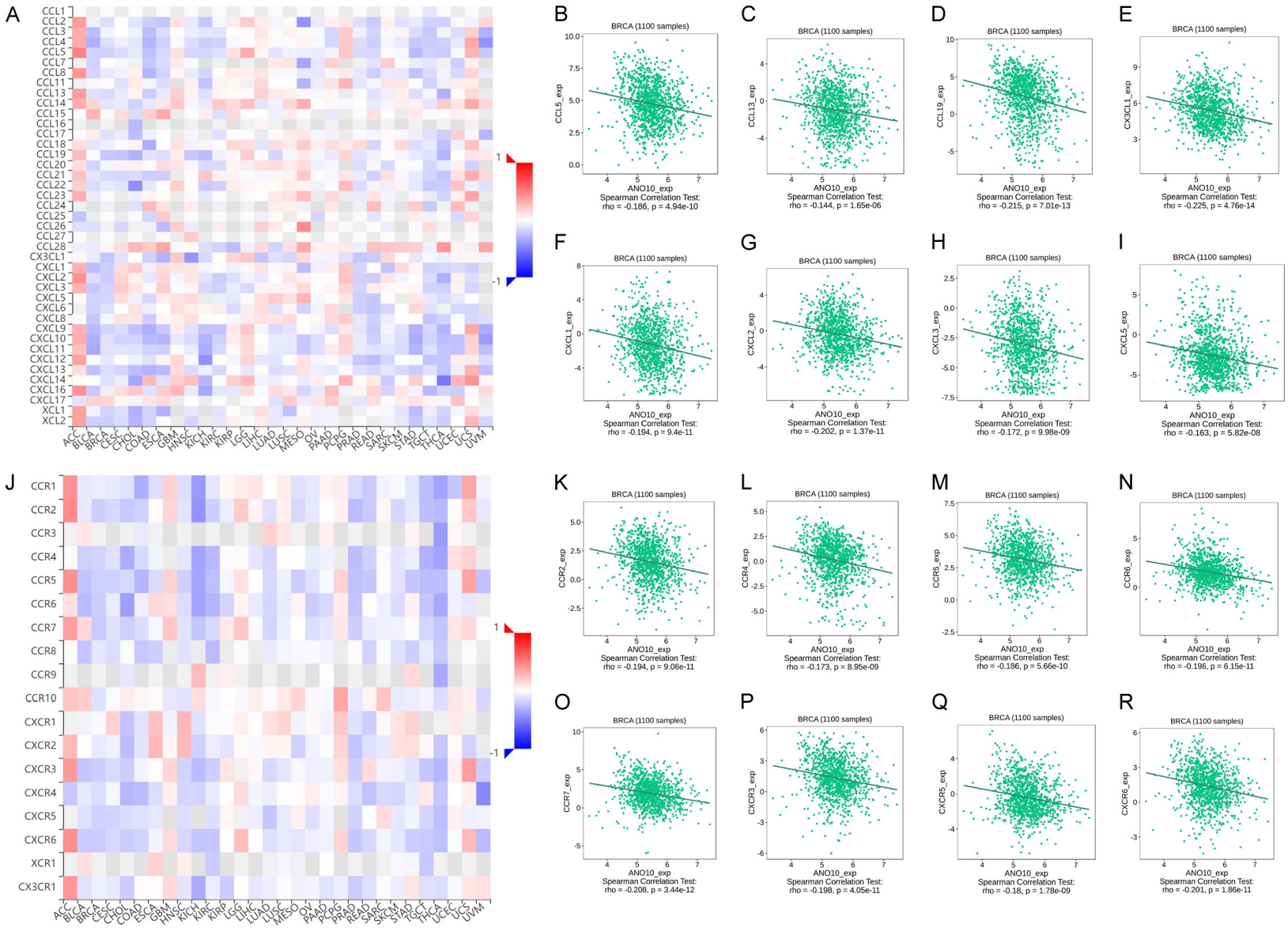

Figure 7. Correlation between ANO10 expression and chemokines or chemokine receptors in BC from the TISIDB database. A. Relevance between ANO10 expression and chemokines in 30 tumors of TCGA database. B-I. Relevance between ANO10 expression and chemokines (CCL5, CCL13, CCL19, CX3CL1, CXCL1, CXCL2, CXCL3 and CXCL5) in the TCGA-BRCA dataset. J. Correlation between ANO10 expression and chemokine receptors in 30 tumors from the TCGA database. K-R. Relevance between ANO10 expression and chemokine receptors (CCR2, CCR4, CCR5, CCR6, CCR7, CXCR3, CXCR5 and CXCR6).

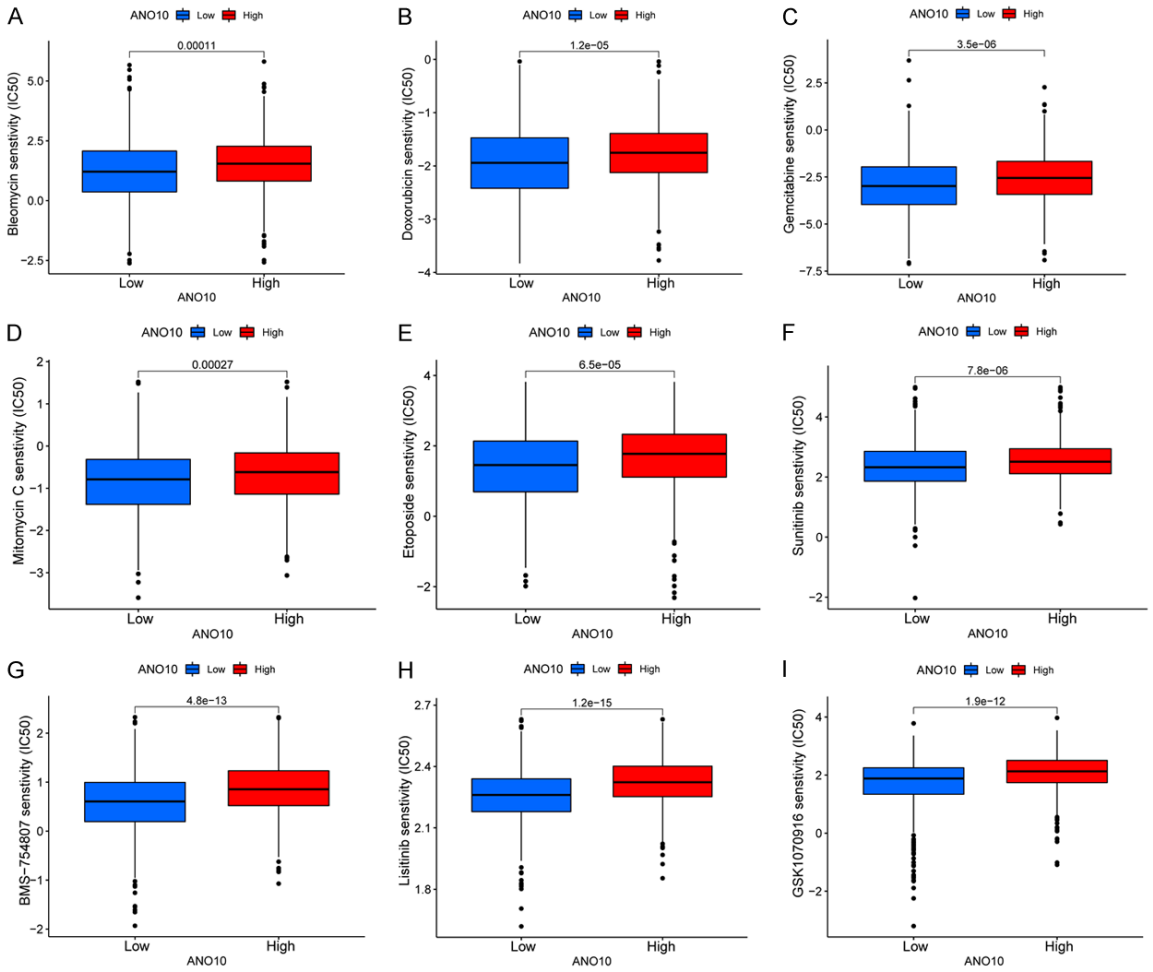

Figure 8. Analysis of drug sensitivity associated with ANO10 expression.

Disclosure of conflict of interest

None.

Address correspondence to: Dr. Jinguo Zhang, Department of Medical Oncology, The First Affiliated Hospital of USTC, Division of Life Science and Medicine, University of Science and Technology of China, Hefei 230000, Anhui, China. ORCID: 0000-0001-9952-9307; E-mail: Zhangjg2022@ustc.edu.cn

References

[1] Hong R and Xu B. Breast cancer: an up-to-date review and future perspectives. Cancer Commun (Lond) 2022; 42: 913-936.

[2] Asleh K, Riaz N and Nielsen TO. Heterogeneity of triple negative breast cancer: current advances in subtyping and treatment implications. J Exp Clin Cancer Res 2022; 41: 265.

[3] So JY, Ohm J, Lipkowitz S and Yang L. Triple negative breast cancer (TNBC): non-genetic tumor heterogeneity and immune microenvironment: emerging treatment options. Pharmacol Ther 2022; 237: 108253.

[4] Perou CM, Sørlie T, Eisen MB, van de Rijn M, Jeffrey SS, Rees CA, Pollack JR, Ross DT, Johnsen H, Akslen LA, Fluge O, Pergamenschikov A, Williams C, Zhu SX, Lønning PE, Børresen-Dale AL, Brown PO and Botstein D. Molecular portraits of human breast tumours. Nature 2000; 406: 747-752.

[5] Sørlie T, Perou CM, Tibshirani R, Aas T, Geisler S, Johnsen H, Hastie T, Eisen MB, van de Rijn M, Jeffrey SS, Thorsen T, Quist H, Matese JC, Brown PO, Botstein D, Lønning PE and Børresen-Dale AL. Gene expression patterns of breast carcinomas distinguish tumor subclasses with clinical implications. Proc Natl Acad Sci U S A 2001; 98: 10869-10874.

[6] Mollah F and Varamini P. Overcoming therapy resistance and relapse in TNBC: emerging

technologies to target breast cancer-associated fibroblasts. Biomedicines 2021; 9: 1921.
[7] Atakpa EC, Thorat MA, Cuzick J and Brentnall AR. Mammographic density, endocrine therapy and breast cancer risk: a prognostic and predictive biomarker review. Cochrane Database Syst Rev 2021; 10: CD013091.
[8] Loi S, Michiels S, Adams S, Loibl S, Budczies J, Denkert C and Salgado R. The journey of tumor-infiltrating lymphocytes as a biomarker in breast cancer: clinical utility in an era of checkpoint inhibition. Ann Oncol 2021; 32: 1236-1244.
[9] Hacking SM, Yakirevich E and Wang Y. From immunohistochemistry to new digital ecosystems: a state-of-the-art biomarker review for precision breast cancer medicine. Cancers (Basel) 2022; 14: 3469.
[10] Hinestrosa MC, Dickersin K, Klein P, Mayer M, Noss K, Slamon D, Sledge G and Visco FM. Shaping the future of biomarker research in breast cancer to ensure clinical relevance. Nat Rev Cancer 2007; 7: 309-315.
[11] Tian T, Zhao Y, Zheng J, Jin S, Liu Z and Wang T. Circular RNA: a potential diagnostic, prognostic, and therapeutic biomarker for human triple-negative breast cancer. Mol Ther Nucleic Acids 2021; 26: 63-80.
[12] Göker E, Hendriks MP, van Tilburg M, Barcaru A, Mittempergher L, van Egmond A, Kleijn M and Generali D. Treatment response and 5-year distant metastasis-free survival outcome in breast cancer patients after the use of MammaPrint and BluePrint to guide preoperative systemic treatment decisions. Eur J Cancer 2022; 167: 92-102.
[13] Pece S, Sestak I, Montani F, Tillhon M, Maisonneuve P, Freddi S, Chu K, Colleoni M, Veronesi P, Disalvatore D, Viale G, Buus R, Cuzick J, Dowsett M and Di Fiore PP. Comparison of StemPrintER with Oncotype DX recurrence score for predicting risk of breast cancer distant recurrence after endocrine therapy. Eur J Cancer 2022; 164: 52-61.
[14] Davodabadi F, Sarhadi M, Arabpour J, Sargazi S, Rahdar A and Díez-Pascual AM. Breast cancer vaccines: new insights into immunomodulatory and nano-therapeutic approaches. J Control Release 2022; 349: 844-875.
[15] Huynh D, Winter P, Märkl F, Endres S and Kobold S. Beyond direct killing-novel cellular immunotherapeutic strategies to reshape the tumor microenvironment. Semin Immunopathol 2022; 45: 215-227.
[16] Zhang J, Pan S, Jian C, Hao L, Dong J, Sun Q, Jin H and Han X. Immunostimulatory properties of chemotherapy in breast cancer: from immunogenic modulation mechanisms to clinical practice. Front Immunol 2021; 12: 819405.
[17] Nakhjavani M and Shigdar S. Future of PD-1/PD-L1 axis modulation for the treatment of triple-negative breast cancer. Pharmacol Res 2022; 175: 106019.
[18] Emens LA, Adams S, Barrios CH, Diéras V, Iwata H, Loi S, Rugo HS, Schneeweiss A, Winer EP, Patel S, Henschel V, Swat A, Kaul M, Molinero L, Patel S, Chui SY and Schmid P. First-line atezolizumab plus nab-paclitaxel for unresectable, locally advanced, or metastatic triple-negative breast cancer: IMpassion130 final overall survival analysis. Ann Oncol 2021; 32: 983-993.
[19] Schmid P, Cortes J, Pusztai L, McArthur H, Kümmel S, Bergh J, Denkert C, Park YH, Hui R, Harbeck N, Takahashi M, Foukakis T, Fasching PA, Cardoso F, Untch M, Jia L, Karantza V, Zhao J, Aktan G, Dent R and O'Shaughnessy J; KEYNOTE-522 Investigators. Pembrolizumab for early triple-negative breast cancer. N Engl J Med 2020; 382: 810-821.
[20] Hahn Y, Kim DS, Pastan IH and Lee B. Anoctamin and transmembrane channel-like proteins are evolutionarily related. Int J Mol Med 2009; 24: 51-55.
[21] Lee B, Hong GS, Lee SH, Kim H, Kim A, Hwang EM, Kim J, Lee MG, Yang JY, Kweon MN, Tse CM, Mark D and Oh U. Anoctamin 1/TMEM16A controls intestinal Cl(-) secretion induced by carbachol and cholera toxin. Exp Mol Med 2019; 51: 1-14.
[22] Sun W, Guo S, Li Y, Li J, Liu C, Chen Y, Wang X, Tan Y, Tian H, Wang C, Du R, Zhong G, Shi S, Ma B, Qu C, Fu J, Jin X, Zhao D, Zhan Y, Ling S, An H and Li Y. Anoctamin 1 controls bone resorption by coupling Cl(-) channel activation with RANKL-RANK signaling transduction. Nat Commun 2022; 13: 2899.
[23] Xu T, Chen M, Xu Q, Xue C, Fu L, Ling K, Hu J and Mei C. Anoctamin 1 inhibition suppresses cystogenesis by enhancing ciliogenesis and the ciliary dosage of polycystins. Front Biosci (Landmark Ed) 2022; 27: 216.
[24] Fukami T, Shiozaki A, Kosuga T, Kudou M, Shimizu H, Ohashi T, Arita T, Konishi H, Komatsu S, Kubota T, Fujiwara H, Okamoto K, Kishimoto M, Morinaga Y, Konishi E and Otsuji E. Anoctamin 5 regulates the cell cycle and affects prognosis in gastric cancer. World J Gastroenterol 2022; 28: 4649-4667.
[25] Heng J, Wu D, Lu S and Zhao Y. miR-106a targets anoctamin 1 (ANO1) to regulate lipopolysaccharide (LPS)-induced inflammatory response in macrophages. Med Sci Monit 2020; 26: e922479.
[26] Vanoni S, Zeng C, Marella S, Uddin J, Wu D, Arora K, Ptaschinski C, Que J, Noah T, Waggoner L, Barski A, Kartashov A, Rochman M, Wen T, Martin L, Spence J, Collins M, Mukkada

V, Putnam P, Naren A, Chehade M, Rothenberg ME and Hogan SP. Identification of anoctamin 1 (ANO1) as a key driver of esophageal epithelial proliferation in eosinophilic esophagitis. J Allergy Clin Immunol 2020; 145: 239-254, e232.

[27] Kim JH, Kim K, Kim I, Seong S, Kim SW and Kim N. Role of anoctamin 5, a gene associated with gnathodiaphyseal dysplasia, in osteoblast and osteoclast differentiation. Bone 2019; 120: 432-438.

[28] Schreiber R, Ousingsawat J and Kunzelmann K. Targeting of intracellular TMEM16 proteins to the plasma membrane and activation by purinergic signaling. Int J Mol Sci 2020; 21: 4065.

[29] Bushell SR, Pike ACW, Falzone ME, Rorsman NJG, Ta CM, Corey RA, Newport TD, Christianson JC, Scofano LF, Shintre CA, Tessitore A, Chu A, Wang Q, Shrestha L, Mukhopadhyay SMM, Love JD, Burgess-Brown NA, Sitsapesan R, Stansfeld PJ, Huiskonen JT, Tammaro P, Accardi A and Carpenter EP. The structural basis of lipid scrambling and inactivation in the endoplasmic reticulum scramblase TMEM16K. Nat Commun 2019; 10: 3956.

[30] Tsuji T, Cheng J, Tatematsu T, Ebata A, Kamikawa H, Fujita A, Gyobu S, Segawa K, Arai H, Taguchi T, Nagata S and Fujimoto T. Predominant localization of phosphatidylserine at the cytoplasmic leaflet of the ER, and its TMEM16K-dependent redistribution. Proc Natl Acad Sci U S A 2019; 116: 13368-13373.

[31] Chamova T, Florez L, Guergueltcheva V, Raycheva M, Kaneva R, Lochmüller H, Kalaydjieva L and Tournev I. ANO10 c.1150_1151del is a founder mutation causing autosomal recessive cerebellar ataxia in Roma/Gypsies. J Neurol 2012; 259: 906-911.

[32] Renaud M, Anheim M, Kamsteeg EJ, Mallaret M, Mochel F, Vermeer S, Drouot N, Pouget J, Redin C, Salort-Campana E, Kremer HP, Verschuuren-Bemelmans CC, Muller J, Scheffer H, Durr A, Tranchant C and Koenig M. Autosomal recessive cerebellar ataxia type 3 due to ANO10 mutations: delineation and genotype-phenotype correlation study. JAMA Neurol 2014; 71: 1305-1310.

[33] Chandrashekar DS, Karthikeyan SK, Korla PK, Patel H, Shovon AR, Athar M, Netto GJ, Qin ZS, Kumar S, Manne U, Creighton CJ and Varambally S. UALCAN: an update to the integrated cancer data analysis platform. Neoplasia 2022; 25: 18-27.

[34] Győrffy B. Survival analysis across the entire transcriptome identifies biomarkers with the highest prognostic power in breast cancer. Comput Struct Biotechnol J 2021; 19: 4101-4109.

[35] Mizuno H, Kitada K, Nakai K and Sarai A. PrognoScan: a new database for meta-analysis of the prognostic value of genes. BMC Med Genomics 2009; 2: 18.

[36] Gao J, Aksoy BA, Dogrusoz U, Dresdner G, Gross B, Sumer SO, Sun Y, Jacobsen A, Sinha R, Larsson E, Cerami E, Sander C and Schultz N. Integrative analysis of complex cancer genomics and clinical profiles using the cBioPortal. Sci Signal 2013; 6: pl1.

[37] Ritchie ME, Phipson B, Wu D, Hu Y, Law CW, Shi W and Smyth GK. Limma powers differential expression analyses for RNA-sequencing and microarray studies. Nucleic Acids Res 2015; 43: e47.

[38] Yu G, Wang LG, Han Y and He QY. ClusterProfiler: an R package for comparing biological themes among gene clusters. OMICS 2012; 16: 284-287.

[39] Newman AM, Liu CL, Green MR, Gentles AJ, Feng W, Xu Y, Hoang CD, Diehn M and Alizadeh AA. Robust enumeration of cell subsets from tissue expression profiles. Nat Methods 2015; 12: 453-457.

[40] Yoshihara K, Shahmoradgoli M, Martínez E, Vegesna R, Kim H, Torres-Garcia W, Treviño V, Shen H, Laird PW, Levine DA, Carter SL, Getz G, Stemke-Hale K, Mills GB and Verhaak RG. Inferring tumour purity and stromal and immune cell admixture from expression data. Nat Commun 2013; 4: 2612.

[41] Ru B, Wong CN, Tong Y, Zhong JY, Zhong SSW, Wu WC, Chu KC, Wong CY, Lau CY, Chen I, Chan NW and Zhang J. TISIDB: an integrated repository portal for tumor-immune system interactions. Bioinformatics 2019; 35: 4200-4202.

[42] Geeleher P, Cox N and Huang RS. pRRophetic: an R package for prediction of clinical chemotherapeutic response from tumor gene expression levels. PLoS One 2014; 9: e107468.

[43] Zhang J, Guan W, Xu X, Wang F, Li X and Xu G. A novel homeostatic loop of sorcin drives paclitaxel-resistance and malignant progression via Smad4/ZEB1/miR-142-5p in human ovarian cancer. Oncogene 2021; 40: 4906-4918.

[44] Thorsson V, Gibbs DL, Brown SD, Wolf D, Bortone DS, Ou Yang TH, Porta-Pardo E, Gao GF, Plaisier CL, Eddy JA, Ziv E, Culhane AC, Paull EO, Sivakumar IKA, Gentles AJ, Malhotra R, Farshidfar F, Colaprico A, Parker JS, Mose LE, Vo NS, Liu J, Liu Y, Rader J, Dhankani V, Reynolds SM, Bowlby R, Califano A, Cherniack AD, Anastassiou D, Bedognetti D, Mokrab Y, Newman AM, Rao A, Chen K, Krasnitz A, Hu H, Malta TM, Noushmehr H, Pedamallu CS, Bullman S, Ojesina AI, Lamb A, Zhou W, Shen H, Choueiri TK, Weinstein JN, Guinney J, Saltz J, Holt RA, Rabkin CS; Cancer Genome Atlas Research Network, Lazar AJ, Serody JS, Demicco

EG, Disis ML, Vincent BG and Shmulevich I. The immune landscape of cancer. Immunity 2018; 48: 812-830, e814.
[45] Viitanen TM, Sukumaran P, Löf C and Törnquist K. Functional coupling of TRPC2 cation channels and the calcium-activated anion channels in rat thyroid cells: implications for iodide homeostasis. J Cell Physiol 2013; 228: 814-823.
[46] Jia L, Liu W, Guan L, Lu M and Wang K. Inhibition of calcium-activated chloride channel ANO1/TMEM16A suppresses tumor growth and invasion in human lung cancer. PLoS One 2015; 10: e0136584.
[47] Liu F, Cao QH, Lu DJ, Luo B, Lu XF, Luo RC and Wang XG. TMEM16A overexpression contributes to tumor invasion and poor prognosis of human gastric cancer through TGF-β signaling. Oncotarget 2015; 6: 11585-11599.
[48] Holstege H, Joosse SA, van Oostrom CT, Nederlof PM, de Vries A and Jonkers J. High incidence of protein-truncating TP53 mutations in BRCA1-related breast cancer. Cancer Res 2009; 69: 3625-3633.
[49] Bethmann D, Feng Z and Fox BA. Immunoprofiling as a predictor of patient's response to cancer therapy-promises and challenges. Curr Opin Immunol 2017; 45: 60-72.
[50] Kramer J and Hawley RS. The spindle-associated transmembrane protein Axs identifies a membranous structure ensheathing the meiotic spindle. Nat Cell Biol 2003; 5: 261-263.
[51] Chen J, Wang H, Peng F, Qiao H, Liu L, Wang L and Shang B. Ano1 is a prognostic biomarker that is correlated with immune infiltration in colorectal cancer. Int J Gen Med 2022; 15: 1547-1564.
[52] Lagarde P, Pérot G, Kauffmann A, Brulard C, Dapremont V, Hostein I, Neuville A, Wozniak A, Sciot R, Schöffski P, Aurias A, Coindre JM, Debiec-Rychter M and Chibon F. Mitotic checkpoints and chromosome instability are strong predictors of clinical outcome in gastrointestinal stromal tumors. Clin Cancer Res 2012; 18: 826-838.
[53] Ousingsawat J, Wanitchakool P, Kmit A, Romao AM, Jantarajit W, Schreiber R and Kunzelmann K. Anoctamin 6 mediates effects essential for innate immunity downstream of P2X7 receptors in macrophages. Nat Commun 2015; 6: 6245.
[54] Hammer C, Wanitchakool P, Sirianant L, Papiol S, Monnheimer M, Faria D, Ousingsawat J, Schramek N, Schmitt C, Margos G, Michel A, Kraiczy P, Pawlita M, Schreiber R, Schulz TF, Fingerle V, Tumani H, Ehrenreich H and Kunzelmann K. A coding variant of ANO10, affecting volume regulation of macrophages, is associated with borrelia seropositivity. Mol Med 2015; 21: 26-37.
[55] Zhang C, Deng Y, Zhang Y, Ba T, Niu S, Chen Y, Gao Y and Dai H. CXCR3 inhibition blocks the nf-κb signaling pathway by elevating autophagy to ameliorate lipopolysaccharide-induced intestinal dysfunction in mice. Cells 2023; 12: 182.
[56] Deng CM, Zhang GG, Liu QW, Xu JJ, Liu ZC, Yang J, Xu TY, Li ZG, Zhang F and Li B. ANO1 reprograms cholesterol metabolism and the tumor microenvironment to promote cancer metastasis. Cancer Res 2023; [Epub ahead of print].
[57] Szteyn K, Schmid E, Nurbaeva MK, Yang W, Münzer P, Kunzelmann K, Lang F and Shumilina E. Expression and functional significance of the Ca(2+)-activated Cl(-) channel ANO6 in dendritic cells. Cell Physiol Biochem 2012; 30: 1319-1332.
[58] Kumar S, Calianese D and Birge RB. Efferocytosis of dying cells differentially modulate immunological outcomes in tumor microenvironment. Immunol Rev 2017; 280: 149-164.
[59] Bao X and Xie L. Targeting purinergic pathway to enhance radiotherapy-induced immunogenic cancer cell death. J Exp Clin Cancer Res 2022; 41: 222.

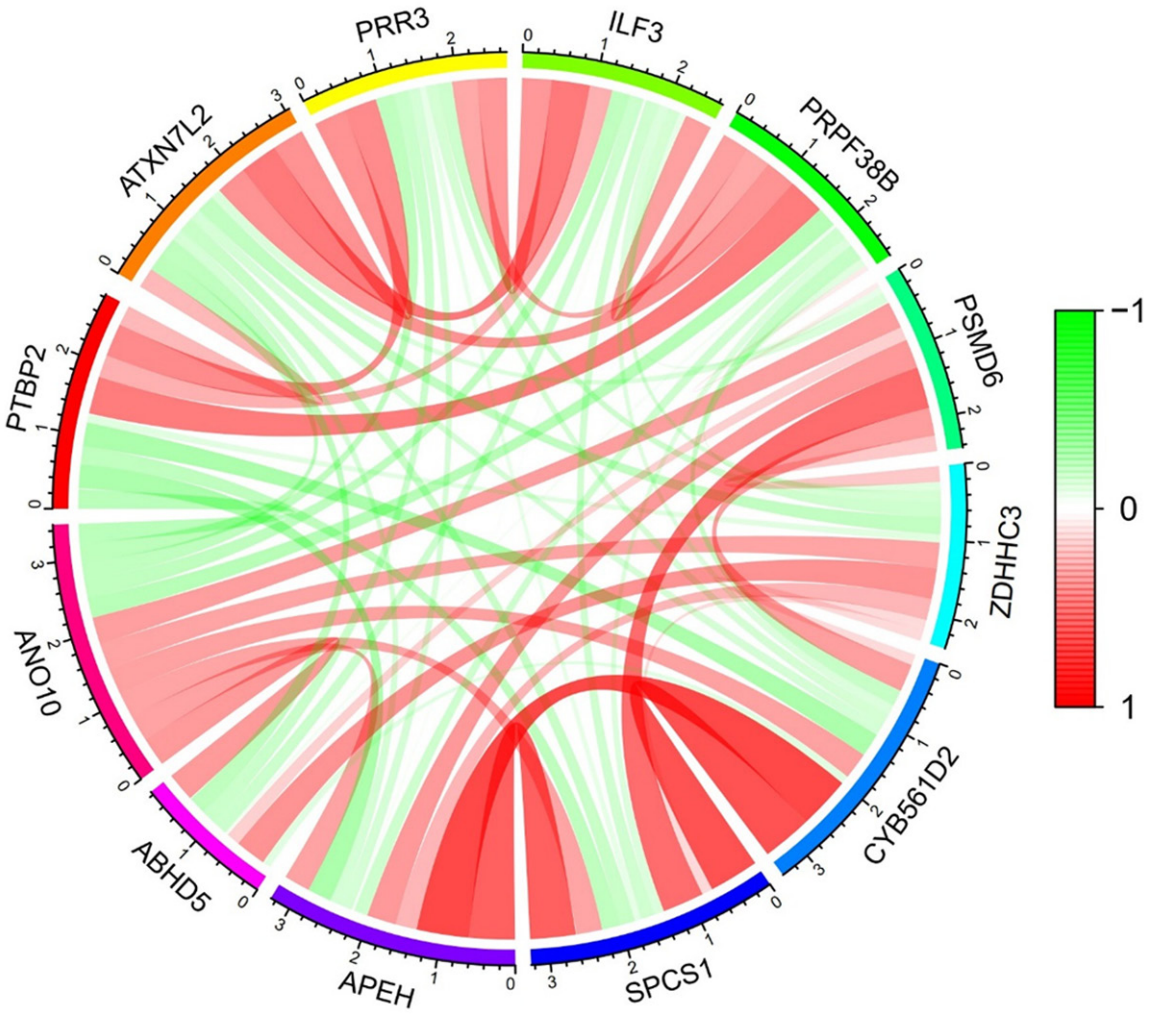

Supplementary Figure 1. Co-expressed genes of ANO10 in breast cancer.

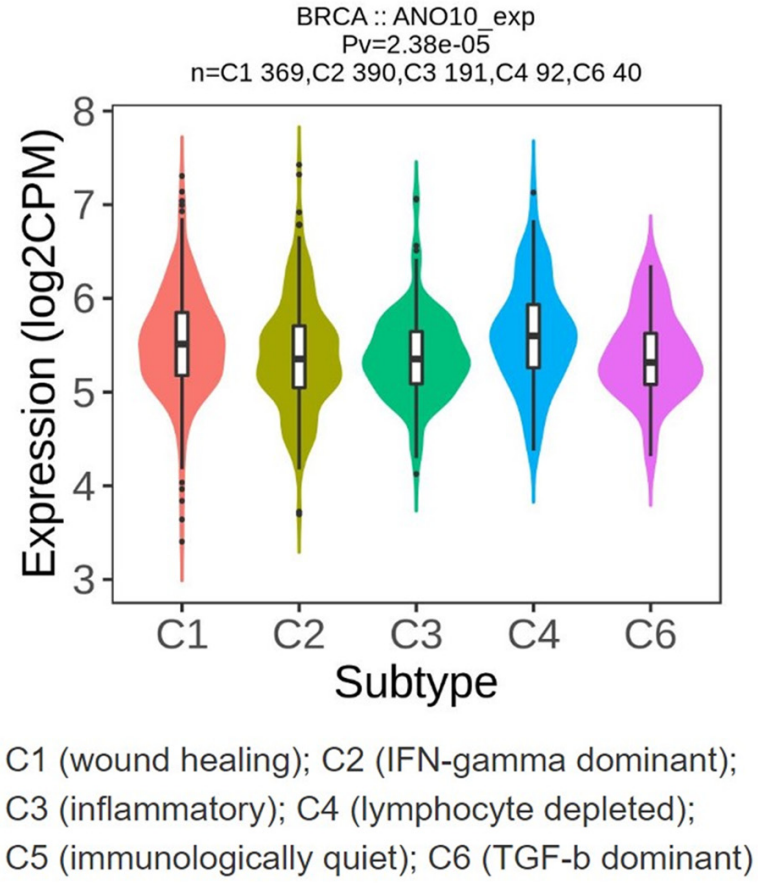

Supplementary Figure 2. The ANO10 expression in different BC subtype defined by Thorsson et al. in TCGA-BRCA dataset.